Biomechanical Modeling to Improve Coronary Artery Bifurcation Stenting

Expert Review Document on Techniques and Clinical Implementation

Antonios P. Antoniadis, MD, PhD,*†‡ Peter Mortier, PhD,§‖ Ghassan Kassab, PhD,¶ Gabriele Dubini, PhD,# Nicolas Foin, PhD,** Yoshinobu Murasato, MD, PhD,†† Andreas A. Giannopoulos, MD,*† Shengxian Tu, PhD,‡‡ Kiyotaka Iwasaki, MD,§§ Yutaka Hikichi, MD,‖‖ Francesco Migliavacca, PhD,# Claudio Chiastra, PhD,#¶¶ Jolanda J. Wentzel, PhD,¶¶ Frank Gijsen, PhD,¶¶ Johan H.C. Reiber, PhD,## Peter Barlis, MBBS, PhD,*** Patrick W. Serruys, MD, PhD,††† Deepak L. Bhatt, MD, MPH,* Goran Stankovic, MD,‡‡‡ Elazer R. Edelman, MD, PhD,*§§§ George D. Giannoglou, MD, PhD,† Yves Louvard, MD,‖‖‖ Yiannis S. Chatzizisis, MD, PhD*†

ABBREVIATIONS AND ACRONYMS

3D = 3-dimensional

CFD = computational fluid dynamics

CT = computed tomography

ESS = endothelial shear stress

ISR = in-stent restenosis

KBI = kissing balloon inflation

From the *Cardiovascular Division, Brigham and Women's Hospital, Harvard Medical School, Boston, Massachusetts; †Cardiovascular Engineering and Atherosclerosis Laboratory, AHEPA University Hospital, Aristotle University Medical School, Thessaloniki, Greece; ‡Cardiovascular Department, Guy's and St Thomas' National Health Service Foundation Trust, London, United Kingdom; §FEops, Ghent, Belgium; ‖IBiTech-bioMMeda, Ghent University, Ghent, Belgium; ¶California Medical Innovations Institute, San Diego, California; #Laboratory of Biological Structure Mechanics (LaBS), Department of Chemistry, Materials and Chemical Engineering "Giulio Natta," Politecnico di Milano, Milan, Italy; **National Heart Centre Singapore, Singapore; ††Department of Cardiology and Clinical Research Institute, Kyushu Medical Center, Fukuoka, Japan; ‡‡Biomedical Instrument Institute, School of Biomedical Engineering, Shanghai Jiao Tong University, Shanghai, China; §§Graduate School of Advanced Science and Engineering, Waseda University, Tokyo, Japan; ‖‖Cardiovascular Division, Department of Internal Medicine, Saga University, Saga, Japan; ¶¶Biomechanics Laboratory, Thoraxcenter, Erasmus University Medical Center, Rotterdam, the Netherlands; ##Division of Image Processing, Department of Radiology, Leiden University Medical Center, Leiden, the Netherlands; ***Melbourne Medical School and Melbourne School of Engineering, The University of Melbourne, Melbourne, Australia; †††International Centre for Circulatory Health, National Heart and Lung Institute, Imperial College London, London, United Kingdom; ‡‡‡Department of Cardiology, Clinical Center of Serbia, and Medical Faculty, University of Belgrade, Belgrade, Serbia; §§§Institute for Medical Engineering and Science, Massachusetts Institute of Technology, Cambridge, Massachusetts; and the ‖‖‖Institut Cardiovasculaire Paris Sud, Massy, France. Supported by Behrakis Foundation, and European Commission, Framework Program 7, Marie Curie International Reintegration Grant, Project: SMILE (249303). Dr. Mortier is a founder and shareholder of FEops. Dr. Tu has received a research grant from Medis. Dr. Reiber is the chief executive officer of and has equity in Medis Medical Imaging Systems. Dr. Bhatt serves on the advisory boards of Cardax, Elsevier Practice Update Cardiology, Medscape Cardiology, Regado Biosciences; serves on the boards of directors of Boston VA Research Institute, Society of Cardiovascular Patient Care; chairs the American Heart Association Get With The Guidelines Steering Committee; serves on the data monitoring committees of Duke Clinical Research Institute, Harvard Clinical Research Institute, Mayo Clinic, Population Health Research Institute; receives honoraria from American College of Cardiology (Senior Associate Editor, *Clinical Trials and News,* ACC.org), Belvoir Publications (Editor in Chief, *Harvard Heart Letter*), Duke Clinical Research Institute (clinical trial steering committees), Harvard Clinical Research Institute (clinical trial steering committee), HMP Communications (Editor in Chief, *Journal of Invasive Cardiology*), *Journal of the American College of Cardiology* (Associate Editor; Section Editor, Pharmacology), Population Health Research Institute (clinical trial steering committee), Slack Publications (Chief Medical Editor, *Cardiology Today's Intervention*), WebMD (continuing medical education steering committees), *Clinical Cardiology* (Deputy Editor); receives research funding from Amarin, AstraZeneca, Bristol-Myers Squibb, Eisai, Ethicon, Forest Laboratories, Ischemix, Medtronic, Pfizer, Roche, Sanofi Aventis, The Medicines Company; and participates in unfunded research for FlowCo, PLx Pharma, and Takeda. Dr. Louvard has received honoraria for workshop participation from Terumo, Abbott, and Medtronic. All other authors have reported that they have no relationships relevant to the contents of this paper to disclose.

Manuscript received March 10, 2015; revised manuscript received June 5, 2015, accepted June 18, 2015.

The advent of coronary artery stents has undoubtedly ushered a new era in interventional cardiology and revolutionized the therapeutic management of patients with coronary artery disease. However, despite significant advances, stents are known to have several shortcomings and more comprehensive insights into the complex in vivo stent-vascular interactions are required. A significant proportion of plaques develop in coronary bifurcation regions, and percutaneous interventions to such lesions account for one-fifth of all coronary interventions (1). Stents in bifurcations exhibit a predisposition to higher rates of in-stent restenosis, thrombosis, and recurrent adverse clinical events (2,3). Therefore, the interventional management of bifurcation lesions remains challenging and the ideal treatment strategy is still elusive.

Locally disturbed blood flow is a major determinant for the development and progression of atherosclerosis (4-6). In particular, low endothelial shear stress (ESS) provokes molecular, cellular, and vascular responses in atherosclerosis-prone sites, leading to plaque initiation and progression toward a more "vulnerable" profile via multiple mechanisms and interactions (7,8). A detailed quantitative appraisal of stent-induced alterations of blood flow following bifurcation stenting plays a key role in understanding this complex geometry (9). This information can facilitate the optimization of bifurcation stenting techniques, stent design, and subsequent reduction of adverse outcomes.

Studies in bifurcation stenting can be classified into computational simulations and in vitro bench testing. Computational simulations extend from idealized simple geometries to more complex anatomical representations of animal- and patient-specific coronary artery geometries obtained from in vivo imaging. Computer simulations can assess the local hemodynamic microenvironment in bifurcations pre- and post-stenting, providing an insight into the role of local hemodynamic stresses on neointimal hyperplasia and stent thrombosis. This review summarizes the current literature on the use of biomechanical modeling approaches to study stent properties, local flow dynamics in stented regions, and outcomes after percutaneous coronary interventions with particular emphasis on bifurcation stenting (**Central Illustration**). Animal studies correlating biomechanical modeling with histopathology findings as well as contemporary advances and challenges in patient-specific modeling for individualized decision making are also discussed.

COMPUTATIONAL SIMULATIONS FOR BIFURCATION STENTING OPTIMIZATION

RATIONALE AND GENERAL CHARACTERISTICS. Computational simulations offer indispensable information into the biomechanical effects of stenting and provide a framework for the quantitative assessment of mechanical stresses and blood flow dynamics in the diseased vascular segment (10-13). Mechanical simulations of stents enable virtual investigation of different bifurcation stenting techniques and can help to evaluate stenting outcomes. Recent advances in hardware and software have boosted the applicability and predictive accuracy of computer simulation studies in bifurcation stenting by diminishing the time required for geometry generation, pre-processing, numerical solution, and post-simulation data processing. Reconstruction of accurate geometries, realistic boundary conditions, and constitutive laws for material properties are essential for accurate computational studies (14). Whereas seminal reports in this field have employed idealized conceptual geometrical models (15,16), patient-specific models based on hybrid clinical coronary imaging data have emerged in the recent years (17-21). Processing of complex arterial geometries to fit a computational grid is not a trivial undertaking. A hybrid meshing method that combines tetrahedral and hexahedral elements has been adopted to reduce

CENTRAL ILLUSTRATION **Biomechanical Modeling of Coronary Artery Bifurcation Stenting**

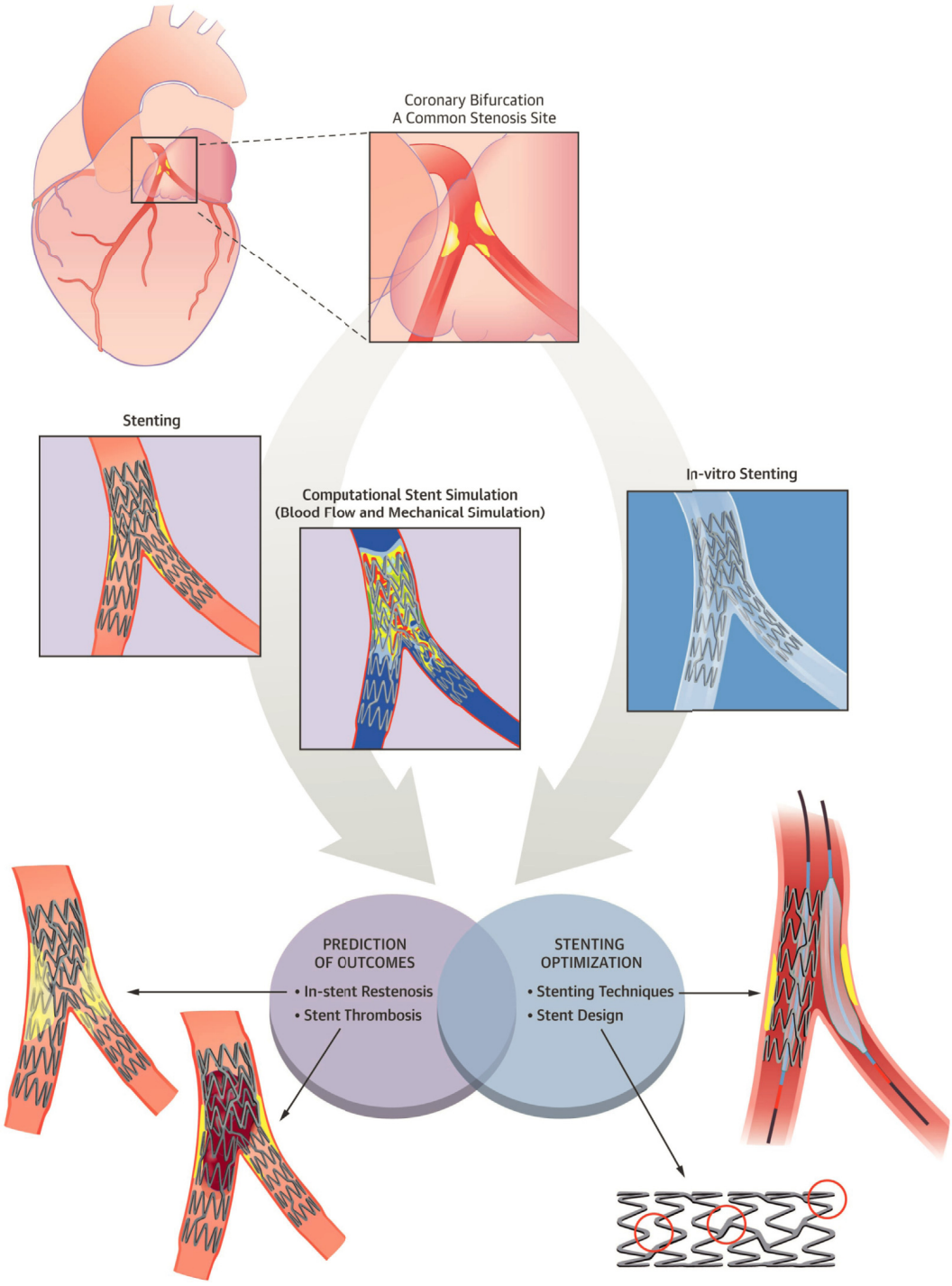

Antoniadis, A.P. et al. J Am Coll Cardiol Intv. 2015; 8(10):1281–96.

Coronary bifurcations are prone to atherosclerosis and common targets of percutaneous coronary interventions. Computational simulations and in vitro bench testing of coronary bifurcation stenting are anticipated to enhance our understanding of the pathophysiology of stent restenosis and thrombosis and facilitate the optimization of stenting techniques and stent design.

computational time when unstructured meshes are employed (22). In general, unstructured meshes are more widely used as they are easier to apply, but structured meshes may accelerate numerical solution and yield more precise results (23). The presence and composition of plaque critically determine the mechanical behavior of the arterial wall and thus the computational simulation results. Plaques exhibit a large variation in their mechanical properties and this is reflected in the constitutive laws used in plaque modeling (24,25). Simplified models are commonly used to study complex and dynamic structural vascular phenomena and interactions (26–28). The mechanical properties of stents and balloons extracted from medical imaging or from manufacturer specifications can also be integrated into the computational models.

COMPUTATIONAL STENT SIMULATIONS FOR STENT DESIGN. Virtual computer testing is an invaluable resource for the early phase design of dedicated bifurcation stent systems. Stent architectures can be evaluated in a virtual manner, thereby significantly reducing time and manufacturing costs. The proof-of-concept and feasibility of this rationale has been demonstrated in computer simulations of prospective novel stents design, which successfully quantified the effects of stent configuration and procedural parameters in stenting outcomes (29).

Moreover, in the current drug-eluting stent era, a sophisticated and proactive understanding of how drug elution occurs in space and time and how much antiproliferative compound can be eluted from the implanted device has become a fundamental issue affecting clinical outcomes. Computer simulations provide important insights in the drug delivery patterns for different stent types and stenting techniques in coronary bifurcations (30,31). As blood circulates around struts, flow streamlines change orientation and acquire secondary components in the radial direction, which affects the transport of molecules to the arterial layers (32). Optimal drug delivery from stent scaffolds is a prerequisite for achieving therapeutic drug concentrations in the wall and at the same time abolishing the occurrence of adverse drug-related side effects. Local pharmacodynamic and pharmacokinetic properties of eluted compounds in association with tissue retention profiles collectively influence the efficacy of drug-eluting stents (33). Comparative computational analyses combining virtual stent implantation, computational fluid dynamics (CFD), and drug release kinetics have reported differences in drug delivery to the main vessel and side branch between different stenting techniques (**Figure 1**) (31,34). This approach yielded useful information, which may be clinically relevant in evaluating the effectiveness of side branch lesion treatment and the influence of incomplete strut apposition and stent overlap on drug delivery.

Although computer simulations may yield high promise in expanding our understanding of bifurcation stenting techniques, certain developmental steps are required to fully unleash its potential in the clinical settings. To date, no clear advantage of dedicated bifurcation stents over conventional stents can be demonstrated on the basis of computer simulations, in vitro bench testing, animal models, and patient-specific modeling. However, performing a simulated bifurcation stenting procedure within a patient-specific model is feasible and attractive. Such computational simulations have been validated against in vitro bench testing and have shown good agreement (35). This approach needs to be further validated using post-interventional in vivo imaging modalities in patients. The automatic and streamlined simulation process in conjunction with recent hardware and software advances is expected to make feasible the study of larger volumes of data in a time-efficient manner.

COMPUTATIONAL STENT SIMULATIONS FOR THE OPTIMIZATION OF KISSING BALLOON INFLATION. Structural simulations have been particularly useful in assessing the outcomes of kissing balloon inflation (KBI) after bifurcation stenting strategies. Previous studies have demonstrated that KBI may cause an elliptic deformation and coating damage of the proximal segment, altered strut configuration, possible arterial injury at the side branch ostium, and high wall stresses that may lead to arterial injury (36,37). Therefore, a minimal balloon overlap was suggested, which would diminish the elliptic deformation after KBI (38). In addition, a short non-compliant balloon in the proximal segment may correct local stent deformation (39). A recent study in 54 computer-simulated stent deployments compared the standard final KBI with a modified approach where the side branch balloon was inflated first and then both balloons were inflated simultaneously with unequal pressures. This study demonstrated that the modified technique for final KBI reduces the elliptical stent deformation in the proximal main vessel and optimizes the side branch access (40). Another study compared KBI against dilation of the main vessel only post single-stent deployment in arterial bifurcations. Both approaches restored an optimal spatial stent configuration in the main vessel and similar side branch access. KBI resulted in higher stresses in the

FIGURE 1 **Computer Simulations of Bifurcation Stenting**

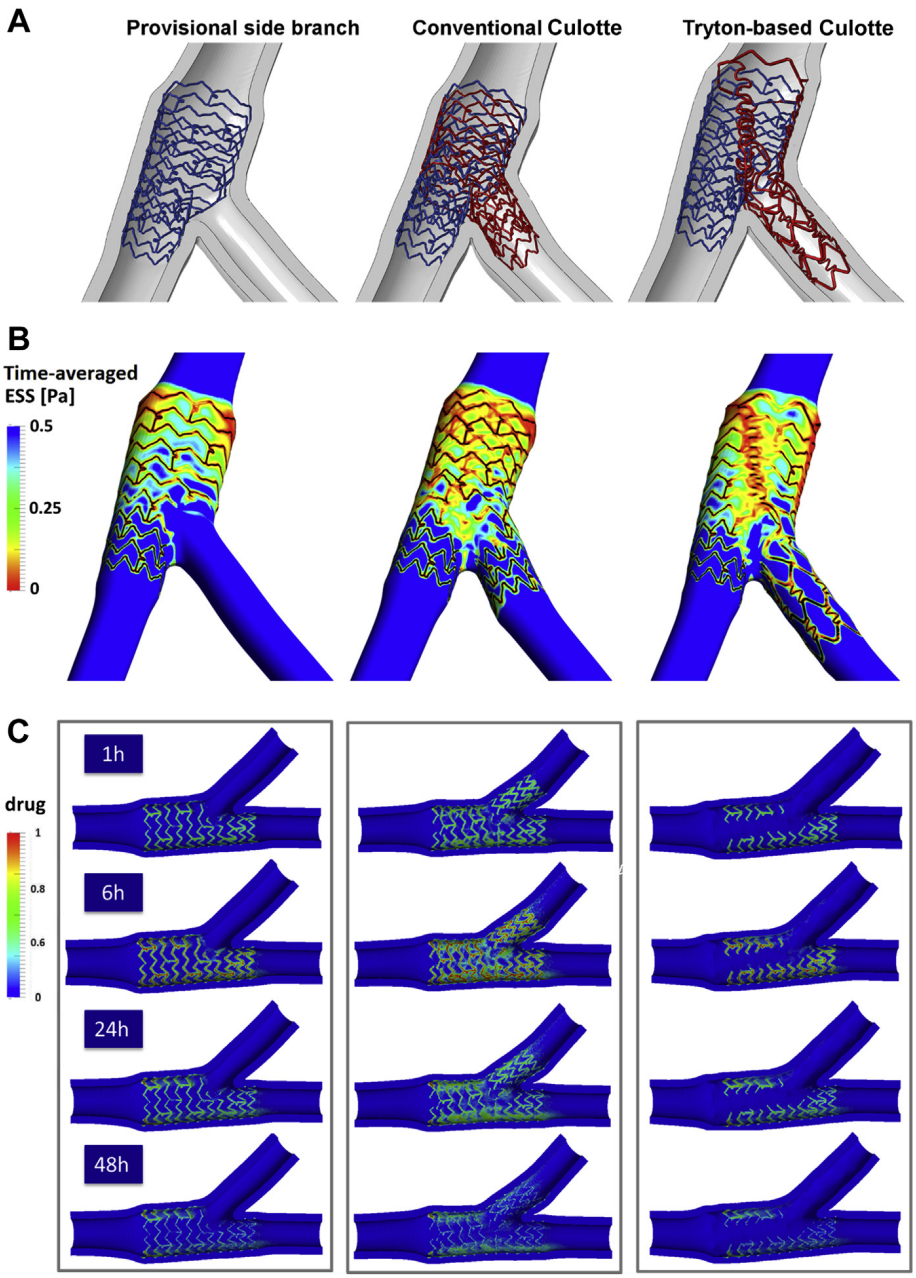

Computational analysis of provisional side branch stenting, conventional culotte, and Tryton-based culotte. **(A)** Virtual stent implantation, **(B)** endothelial shear stress (ESS) calculation, **(C)** drug release analysis. Low ESS regions are denoted in **red**. The drug distribution in the arterial wall of the coronary bifurcation was evaluated at 4 time points (1 h, 6 h, 24 h, 48 h) for each stenting technique. Reprinted with permission from Morlacchi et al. (31). Pa = Pascal.

arterial wall during balloon inflation, making it less favorable in a single-stent strategy (28).

Computer structural simulations were also used to investigate the biomechanical influence of the final KBI in provisional side branch stenting. Stresses generated in the arterial wall by stent expansion and hemodynamic forces on the intimal layer of the vessel were examined before and after KBI. KBI resulted in

almost 2.5× higher average wall stress than stent deployment in the main vessel only. KBI was favorable, however, with respect to local blood flow patterns for the side branch. Based on these simulations, a new tapered balloon dedicated to bifurcation lesions was proposed to limit the structural damage induced to the arterial wall and to enhance the local ESS patterns (41).

Another study investigated the local hemodynamic effects of KBI when access is performed through proximal or distal side of the side branch (22). The study showed that access of the side branch through stent cells on the distal side of the side branch led to a smaller area exposed to low ESS compared with access to the proximal side of the side branch. This finding provides the theoretical foundation to the clinical experience of accessing the distal side of the side branch when the provisional stenting strategy is followed by KBI.

COMPUTATIONAL MODELING OF IN-STENT RESTENOSIS AND STENT THROMBOSIS. Blood flow properties in stented arterial segments contribute significantly to the clinical outcomes following stenting. It has been shown that low ESS, flow recirculation, and stagnation decrease convective flux in the arterial wall, resulting in local accumulation of biologically active compounds (42–44). In animal models, areas of low ESS between stent struts were associated with more pronounced neointimal hyperplasia (45,46). In humans, in-stent low-ESS regions colocalized with increased neointimal thickness in bare-metal stents and low ESS was associated with neointimal thickness in drug-eluting stents (47). Bifurcation lesions more frequently develop in-stent restenosis (ISR) as a result of geometrical complexities causing disturbed flow patterns (8). Stent placement per se further exacerbates the adverse hemodynamic microenvironment with strut dimensions and shape, directly influencing the flow parameters and affecting stent outcomes (43,48). Increased stent diameter relates to ISR (49), and this likely occurs not only by inducing arterial injury but also by creating a slow-flow environment within the stent with low local ESS. Notably, stent underexpansion also favors ISR as it adversely affects local ESS by creating small gaps between the struts and the arterial wall and increasing flow resistance (46). Stent overlap also relates to poor stent outcomes, and this effect might be due to the unfavorable hemodynamic conditions created locally in the overlapping stent segments (7,50).

In addition to the well-known effects of ESS on the endothelium, the wall stresses within the wall may also play an important role in vessel injury and remodeling (51). The stent struts cause stress concentrations as well as static stresses and strain in the vessel wall that can lead to vessel injury, inflammation, and cellular proliferation (52). It is plausible that the biomechanical stresses act in synergy (53). An inverse relation between ESS and neointimal hyperplasia and a linear relation between wall stress and neointimal hyperplasia were found. Of note, a linear association between the ratio of wall stress to ESS and neointimal hyperplasia was noted, suggesting that both fluid and solid mechanics influence the extent of neointimal hyperplasia (53).

IN VITRO BENCH TESTING FOR BIFURCATION STENTING OPTIMIZATION

RATIONALE AND GENERAL CHARACTERISTICS. In vitro bench testing of bifurcation stenting involves the deployment of 1 or more stents within an artificial bifurcation model and visualization of the subsequent deformations of the lumen and stent. Studies of this type have been extensively used to improve our understanding of bifurcation stenting techniques for many years (1,54,55). This investigational approach illustrates the realistic configuration of the complex bifurcation stenting techniques with clear visualization using high-resolution invasive imaging (e.g., optical coherence tomography, intravascular ultrasound) or noninvasive imaging (e.g., charge-coupled device camera, endoscopy, scanning electron microscopy, and micro-computed tomography (micro-CT) (56,57). Micro-CT provides clear images with resolutions of 10 to 20 μm to enable a detailed inspection of stent configuration, an impact of post-dilation on stent deformations, and an evaluation of different stenting techniques in a controlled and reproducible environment. The images acquired are processed to allow volume rendering, geometry rotation, cut-plane views, and fly-through animations. Unlike clinical imaging modalities, in vitro bench testing provides a thorough assessment of stent deformations, strut apposition, and vascular scaffolding. Furthermore, integration with CFD provides insights into the flow disturbances that may account for the higher rates of restenosis and thrombosis in coronary bifurcations.

In recent years, considerable progress has been achieved in construction of anatomically accurate in vitro bifurcation models. The initial rigid polymethyl methacrylate phantoms were replaced by flexible silicone models. Also, the conventional planar bifurcation models were gradually surrogated

FIGURE 2 In Vitro Bench Testing of Bifurcation Stenting

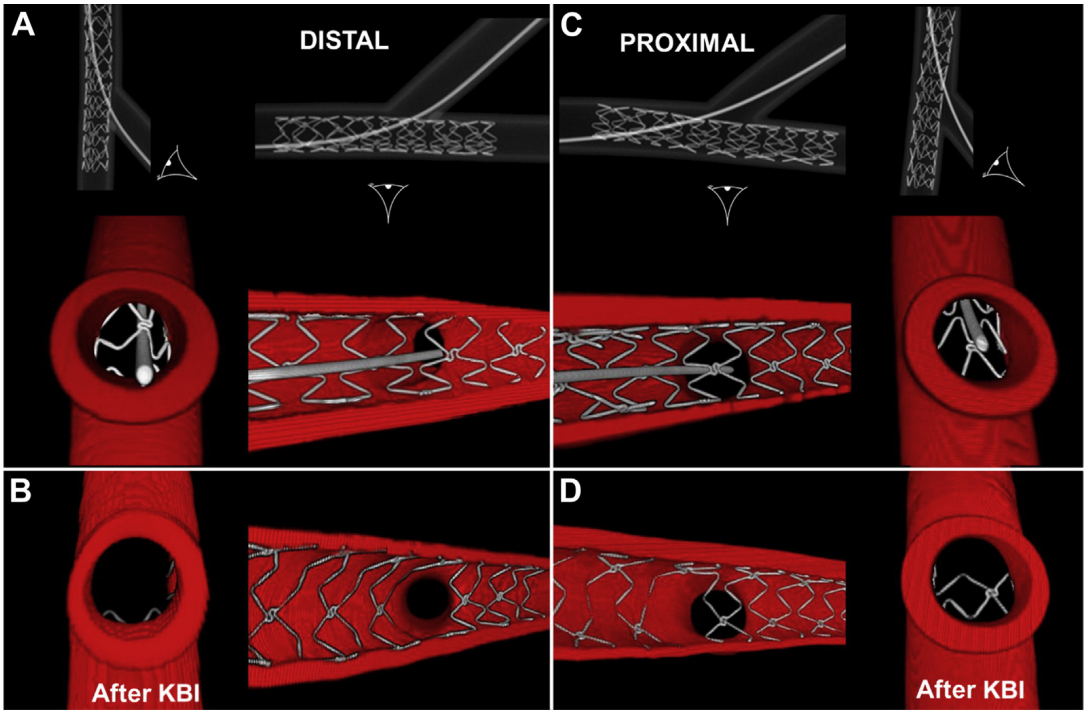

This figure highlights the importance of crossing the side branch through a distal cell of the main vessel stent to achieve good side branch ostial opening after final kissing balloon inflation (KBI). Crossing the guidewire through a distal stent cell **(A)** optimizes the side branch ostial area **(B)**, whereas crossing through a proximal stent cell **(C)** leaves malapposed struts near the carina **(D)**. Adapted with permission from Foin et al. (65).

by 3-dimensional (3D)-structured geometries created by rapid prototyping technology. These 3D models resemble the true arterial shape and take into account the physiologic tapering in arterial dimensions from proximal to distal locations, thereby representing more closely the real vascular configuration (58).

IN VITRO BENCH TESTING FOR THE OPTIMIZATION OF SIDE BRANCH RECROSSING, CRUSH, AND CULOTTE STENTING. The characteristics of blood flow in the left main bifurcation were assessed in a 3D silicone model adopted from a patient-specific artery featuring similar elasticity and compliance. Flow delay was noted at the lateral wall area (which was more prominent in the distal post-stenotic segment) and high flow at the flow-divider region. Mini-crush stenting restored flow patterns at the lateral walls but created new flow disturbance at the carina in the area lacking strut coverage and in the overdilated area close to the main vessel ostium (59). Interestingly, it has been reported that when the diseased side branch is patent in a bifurcation lesion, the magnitude of ISR in the main vessel is higher than when the side branch is occluded (60). This observation may be explained by the adverse local hemodynamics that the side branch flow introduces and can conceptually account for the nonapparent clinical benefit after double stenting of bifurcation lesions (61,62).

The optimal side branch ostial dilation through the main vessel stent is critical to the overall stenting results in bifurcation regions (63,64). In vitro testing showed that the location of wire crossing in the main vessel stent largely affects the outcomes of side branch ostial dilation (64), and the current recommendation is to recross through a distal cell of the main vessel stent (39). Crossing through a proximal cell results in unapposed struts in front of the carina, reduction of the struts-free side branch ostial area, and suboptimal scaffolding of the side branch ostium (**Figure 2**) (56,58,65). The use of optical coherence tomography to confirm the site of wire recrossing significantly reduces the rate of strut malapposition

FIGURE 3 In Vitro Bench Testing of Bifurcation Stenting

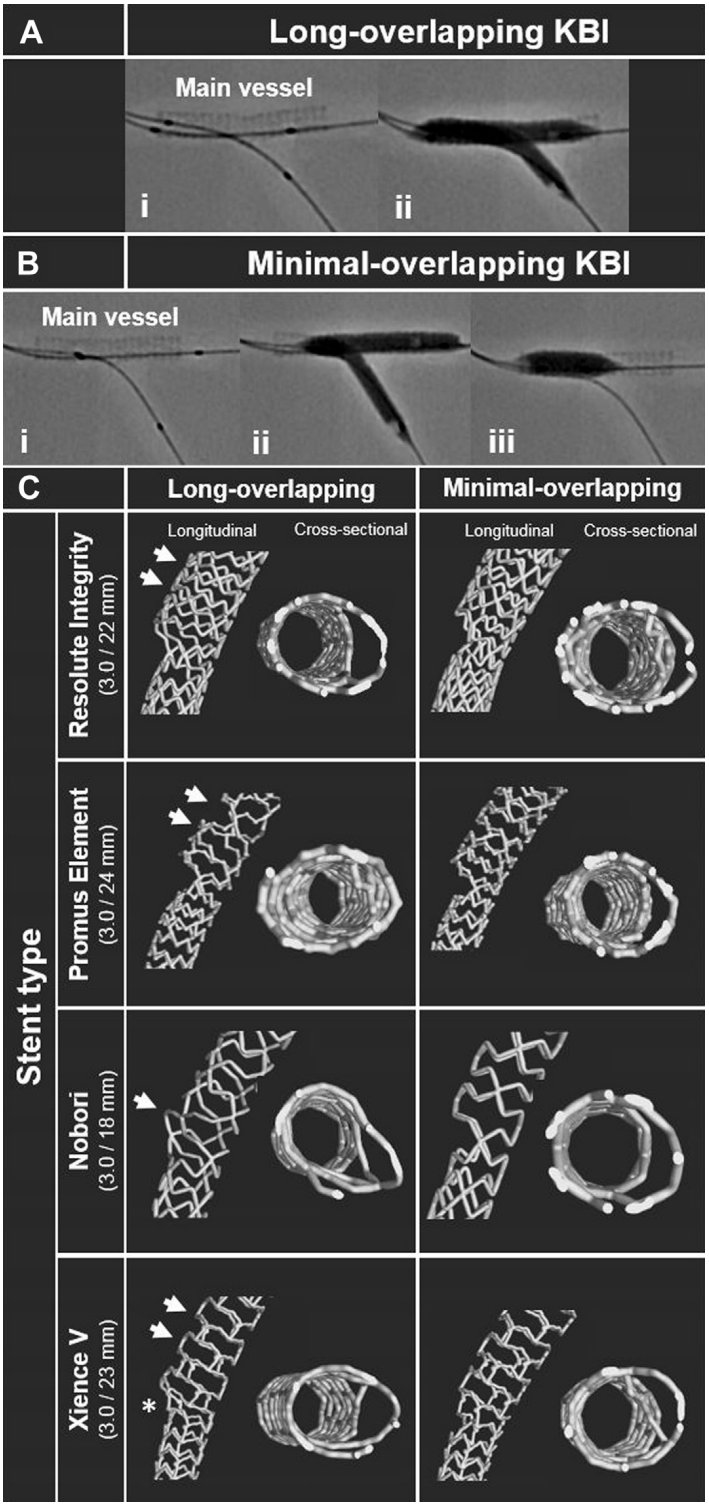

Continued on the next page

in these settings (66). However, in the case of crush stenting, in vitro bench testing suggests that distal cell recrossing should not be pursued as it induces gaps in stent scaffolding of the side branch. These gaps are the result of the guidewire following a short course outside the side branch stent mesh before entering the side branch stent area (58).

In vitro bench testing yielded important information for the optimization of culotte stenting. Culotte stenting is more appropriate in stents with an open-cell-based architecture. In stent cells that cannot be sufficiently enlarged, the use of a balloon that exceeds the maximum stent diameter leads to "napkin ring" stent deformation (i.e., restriction of stent expansion at the side branch ostium) (57).

IN VITRO BENCH TESTING FOR THE OPTIMIZATION OF KBI. In vitro models have been successfully used to assess the best strategy for post-stenting KBI in bifurcation regions. In a 3D left main bifurcation model, differences in stent morphology were found between long-overlapping and minimal-overlapping KBI followed by proximal optimization (**Figure 3**) (67). The differences were variable but specific for each stent type. Another bench study demonstrated that a 2-step KBI after crush stenting (i.e., where a high pressure post-dilation in the side branch is followed by simultaneous KBI) significantly reduced the residual ostial stenosis compared with using single KBI (58). Bifurcation in vitro stent models are particularly useful in the assessment and prevention of strut malapposition after KBI (68-70). During KBI, the aggregate diameter of the 2 overlapping balloons can exceed the main vessel reference diameter and elicit an asymmetric stent expansion that can lead to arterial overstretch and stent distortion in the proximal main vessel (68,69). In vitro bench studies also showed that sequential dilation of the side branch and main vessel may be a possible alternative to KBI (**Figure 4**) (54,69).

LIMITATIONS AND CHALLENGES OF IN VITRO BENCH TESTING. In vitro bench testing has the advantage of providing a realistic assessment of the bifurcation geometry and stent properties and can be applied in large-scale studies (58). However, there are several shortcomings that necessitate further consideration: 1) differences in elasticity between in vitro vascular models and human coronary arteries; 2) difficulty in the generation of an accurate atherosclerotic coronary model with variable luminal stenosis, plaque burden, and wall calcification; 3) incomplete representation of the complex 3D

structure of coronary bifurcations; and 4) insuffi-cient representation of the effects of coronary artery motion and deformations during the cardiac cycle on bifurcation models, which precludes the investigation of the temporal strut deformations with increasing inflation pressure. Furthermore, a widespread application of micro-CT imaging has significant financial and time-related constraints.

The development of more advanced, patient-specific modeling approaches aims to address these limitations. Three-dimensional printing can produce accurate models of the coronary vasculature in-cluding bifurcations of any shape using materials that have similar properties to the arterial wall (71). Investigation of stent types, stenting techniques, and outcomes in these realistic geometries are anticipated to shed further light on optimal approaches for bifurcation stenting.

BRIDGING THE GAP BETWEEN MODELS AND HISTOLOGY: ANIMAL STUDIES

Animal studies provide a unique opportunity to explore the association of stent modeling data with real tissue pathology as examined by histological methods. Specifically, porcine animal models were used to investigate the association between locally disturbed flow and neointimal hyperplasia after stenting. Studies demonstrated that the localization of in-stent neointimal hyperplasia follows the pattern of boundary layer separation seen in in vitro models (i.e., the lesions form immediately distal to the ostium of the side branch and are highly eccentric, with a maximum thickness at the lateral wall of the main vessel). Histopathology assessment revealed 2 distinct cellular regions within the stent: 1) an inner annular region (200 to 300 μm) populated by dense smooth muscle cells; and 2) an outer crescentic region that is more prominent at the lateral wall, rich in fibrin, and exhibiting neovascularization (**Figure 5**) (60).

A study in swine coronary arteries evaluated the use of micro-CT imaging in the assessment of the morphology and configuration of a dedicated bifurcation stenting system (72). The proximal diameter and area of the stents were higher than the respective values for the distal stent edge and not very different than the manufacturer's values. The stent length was shorter than the length provided by the manufacturer in the majority of cases. This study highlighted the use of micro-CT imaging for accurate visualization of stent morphology and 3D configuration in bifurcations regions and may have important implications in stent design.

PATIENT-SPECIFIC COMPUTER MODELING OF BIFURCATION STENTING

There is no doubt that both blood flow and solid mechanics of the coronary arterial wall strongly rely on vascular geometry. For this reason, an accurate reconstruction of the patient-specific 3D geometry for percutaneous coronary intervention is warranted. In vivo coronary imaging is a particularly challenging endeavor since small arterial caliber, 3D spatial tortuosity, and cardiac motion create practical challenges. Although coronary angiography has traditionally been the most widely used method for coronary imaging, other methods have emerged, such as intravascular ultrasound, optical coherence tomography, coronary computed tomography angiography, and magnetic resonance imaging. Novel imaging modalities, in particular optical coherence tomography, offer high-resolution imaging of the coronary lumen and assessment of the composition of the superficial plaque components, thereby serving as the basis for more realistic CFD models and insightful experimental investigations (73).

The various invasive and noninvasive methods are complementary and collectively provide additional information with regard to lumen shape, 3D anatomy, plaque dimensions and composition, as well as stent dimensions and strut position. Various combinations of the preceding methods (hybrid imaging) are able to produce highly accurate 3D reconstructions of the coronary arteries to enable more realistic CFD analyses, structural mechanical simulations, and

FIGURE 3 Continued

Micro-computed tomography (micro-CT) study of the differences between long-overlapping kissing balloon inflation (KBI) and minimal-overlapping KBI after implantation of 4 new-generation drug-eluting stents (Resolute Integrity 3.0/22 mm, Medtronic, Santa Rosa, California; Promus Element 3.0/24 mm, Boston Scientific, Natick, Massachusetts; Nobori 3.0/18 mm, Terumo, Tokyo, Japan; and Xience V 3.0/23 mm, Abbott Vascular, Santa Clara, California) in an in vitro model of left main bifurcation. **(A)** In the long-overlapping approach, the stent balloon and a 3.0/15 mm post-dilation balloon were positioned at the proximal stent edge **(i)** and inflated simultaneously **(ii)**. **(B)** In the minimal-overlapping approach, both balloons were positioned just proximal to the bifurcation **(i)** and inflated simultaneously **(ii)**. The proximal main vessel was optimized with a 4.0/10 mm balloon **(iii)**. Reprinted with permission from Murasato et al. (67). **(C)** Resolute Integrity: Long-overlapping KBI led to less strut dilation at the proximal main vessel compared with Promus Element and Nobori **(arrows)**. Promus Element: Long-overlapping KBI led to longitudinal stent strut deformation **(arrows)**. Nobori: Long-overlapping KBI led to oval-shaped dilation of the main vessel stent at the bifurcation region **(arrow)**. Xience V: Long-overlapping KBI maintained the 3-link structure of the stent at the proximal main vessel **(arrows)** and induced inadequate strut expansion at the ostium of the side branch **(asterisk)**. Cross-sectional views demonstrate more oval-shaped dilation of the main vessel stent at the bifurcation with long-overlapping KBI compared with minimal-overlapping KBI in each stent type (courtesy of Dr. Murasato).

FIGURE 4 In Vitro Bench Testing of Bifurcation Stenting

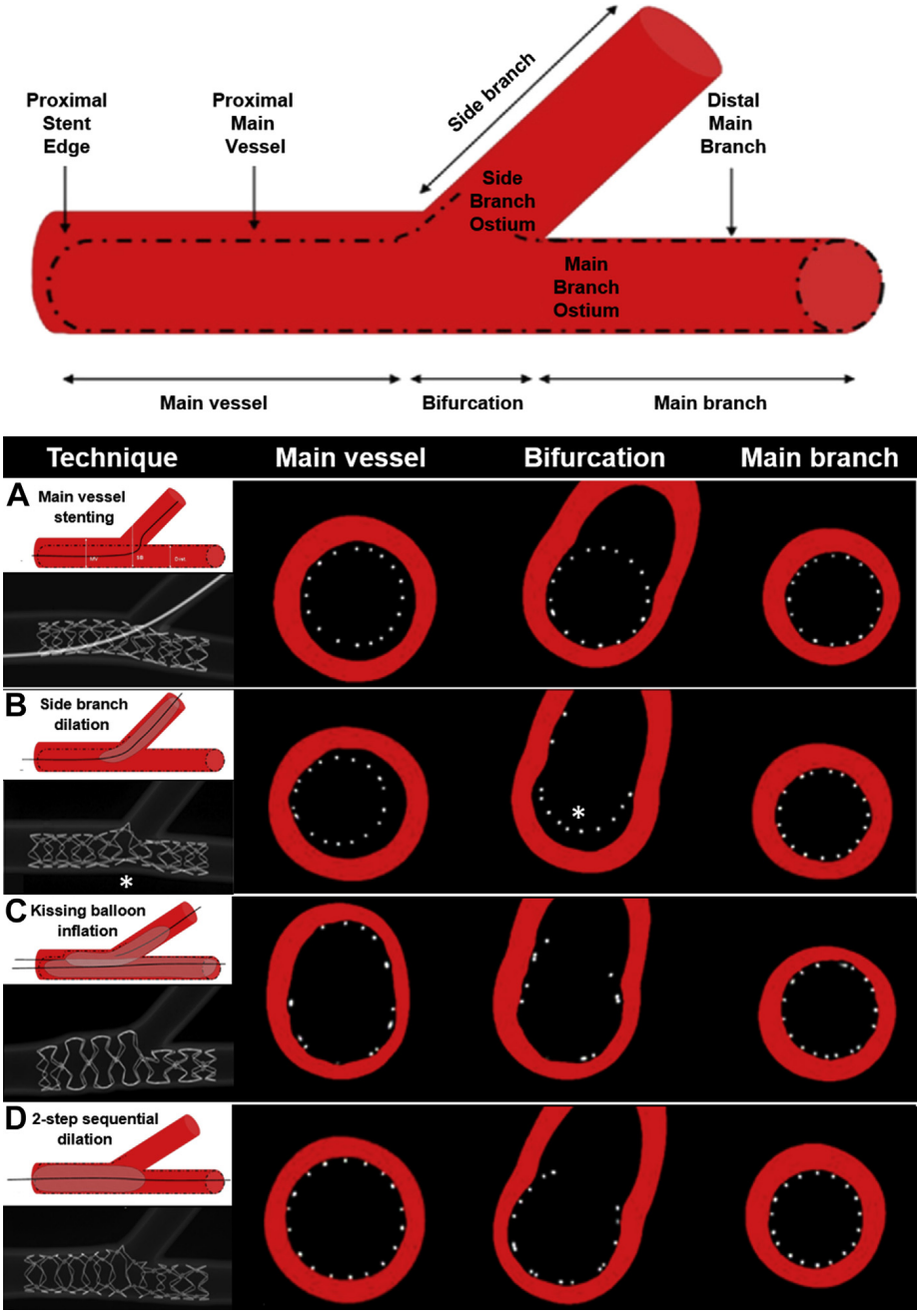

Bench model testing to facilitate optimization of bifurcation stenting. **(A)** Deployment of a stent in the main vessel of the bifurcation model and incomplete stent apposition proximal and at the side branch ostium. **(B)** Dilation of the side branch with a 2.5-mm noncompliant balloon produces a risk of malapposition opposite to the ostium of the side branch **(asterisk)**. **(C)** Kissing balloon inflation with a 3.0-mm balloon in the main vessel and a 2.5-mm balloon in the side branch simultaneously inflated at 10 atm. **(D)** Two-step sequential post-dilation of main vessel with a 3.75-mm noncompliant balloon after side branch dilation. Adapted with permission from Foin et al. (69).

fluid-structure interaction models (17,74-77). However, the simultaneous reconstruction of both the artery and the stents in in vivo settings is still not straightforward. Currently, only optical coherence tomography permits a simultaneous clear visualization of both the arterial wall and stents in vivo and such methods of reconstructing true bifurcation geometry are still under development (**Figure 6**) (78-80).

FIGURE 5 **Animal Studies of Bifurcation Stenting**

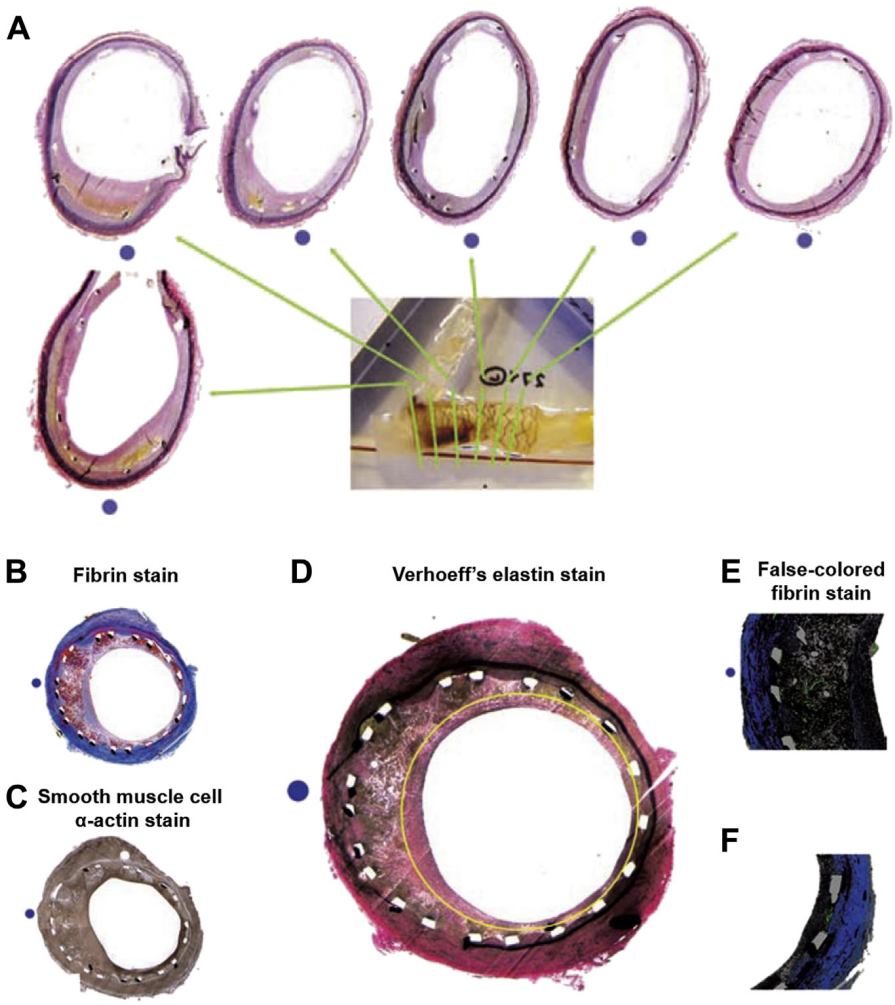

Study of in-stent restenosis after bifurcation stenting in a porcine model. **(A)** Serial cross sections along the bifurcation showing neointimal hyperplasia along the lateral wall **(blue dots)**. **(B)** Representative cross section showing high concentration of fibrin around the stent struts, particularly on the lateral wall. **(C)** Smooth muscle cell α-actin immunostaining showing abundant smooth muscle cells inside along the lumen circumference (dense **brown** area). **(D)** Verhoeff's elastin immunostaining shows a cellular, dense region of relatively uniform thickness (inside **yellow circle**) and an extracellular matrix-rich crescent region across the lateral wall. **(E, F)** False-colored enhancement of fibrin concentration **(green)** highlights the increased neointimal hyperplasia at the lateral wall **(E)** versus at the flow divider **(F)**. Adapted with permission from Richter et al. (60).

For the particular case of bifurcation lesions, the 3D geometry reconstruction is more efficiently accomplished via coronary CT angiography (81). The accuracy of CT-derived coronary lumen area in comparison to intravascular ultrasound has recently been validated in humans (82). The image segmentation and cross-sectional area extraction algorithm for reconstruction of coronary arteries proved to be accurate enough for the determination of vessel and lumen area, providing fundamental morphometric data for patient-specific models to diagnose and treat coronary artery disease. There are a number of challenges that need to be addressed in future CT angiography clinical studies: 1) image quality influences the automatic segmentation and can result in errors; 2) lesion appearance in the vasculature can vary in intensity depending on plaque constitution and can in turn affect image quality; 3) a uniform threshold for segmentation is not straightforward in CT images; and 4) disconnected

FIGURE 6 In Vivo Patient-Specific Modeling of Bifurcation Stenting

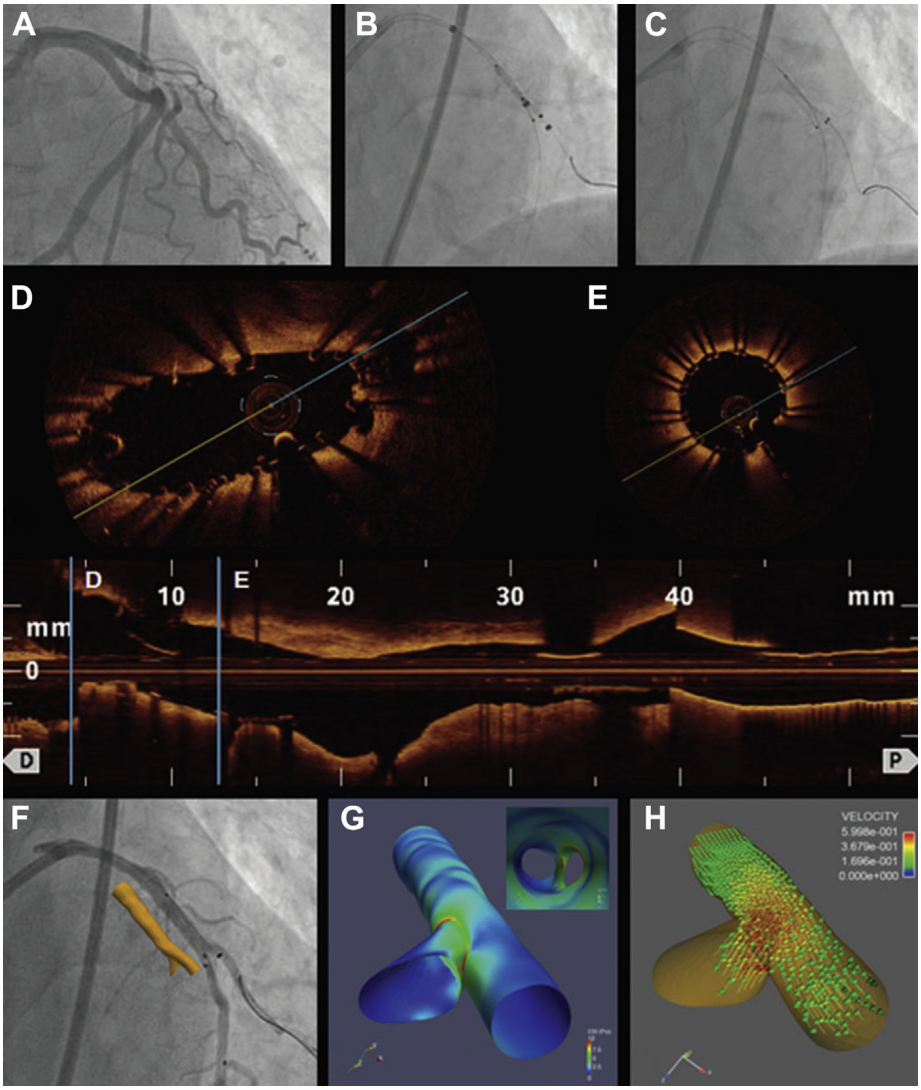

In vivo optical coherence tomography-based 3-dimensional (3D) reconstruction of bifurcation stenting in man. **(A)** Coronary angiography demonstrates a lesion in the left anterior descending artery and first diagonal branch bifurcation. **(B, C)** Implantation of a self-expanding dedicated bifurcation stent with an abluminal biodegradable coating (Axxess, Biosensors International, Morges, Switzerland). **(D, E)** Optical coherence tomography evaluation of the final result. **(F)** 3D reconstruction of the stented bifurcation. **(G, H)** Endothelial shear stress (ESS) and blood velocity distribution in the 3D reconstructed bifurcation showing that ESS and flow velocity are higher at the carina and lower at the lateral walls. Reprinted with permission from Antoniadis et al. (78).

gaps can create unsmoothness of vessels, and automatic and manual correction of gaps is needed.

The introduction of numerical simulations of mechanical stresses and flow in patient-derived arterial geometries can significantly contribute to the clinical translation of the early phase experimental studies. Preliminary reports show the biomechanical influence of stents deployment in the coronary bifurcations during and after stenting procedures. In particular, the straightening of the arterial wall and the influence of 2 overlapping stents significantly affects the stress fields. The presence of overlapping devices proved to have major impact on both local structural and hemodynamic parameters (**Figure 7**) (18,19).

Accurate reproduction of patient-specific coronary anatomy in the complex bifurcation regions is

feasible but currently requires a hybrid imaging approach combining the fusion and combination of multiple modalities. In terms of the translation of preclinical findings in patient-oriented outcomes, randomized clinical trials comparing stent geometries and stenting techniques with respect to subsequent stent restenosis and thrombosis are warranted. Such studies should include discrete baseline and follow-up assessments. At baseline, combined pre-intervention coronary imaging (either noninvasive or invasive) with immediate post-intervention imaging is required. Pre-intervention imaging can be used for stenting simulations, whereas post-intervention imaging can be used for CFD and structural analysis of the stented arteries for correlation with outcome. At follow-up, detailed assessment of stent parameters as well as clinical outcomes will identify cases of ISR and stent thrombosis leading to adverse events. Integration of this data and analysis will enable the identification of local biomechanical factors that contribute to the clinical outcomes and therefore set the stage for improved clinical decision making by the physicians. Although such studies demand resources and effort, the expected clinical benefits may justify the investment.

CONCLUSIONS AND FUTURE PERSPECTIVES

Modeling approaches appear to be a fundamental component toward the consummation of techniques and devices for coronary bifurcation interventions. Computer simulations and in vitro bench testing have the potential to complement the in vivo morphological (intravascular ultrasound, optical coherence tomography) and functional (fractional flow reserve)

FIGURE 7 In Vivo Patient-Specific Modeling of Bifurcation Stenting

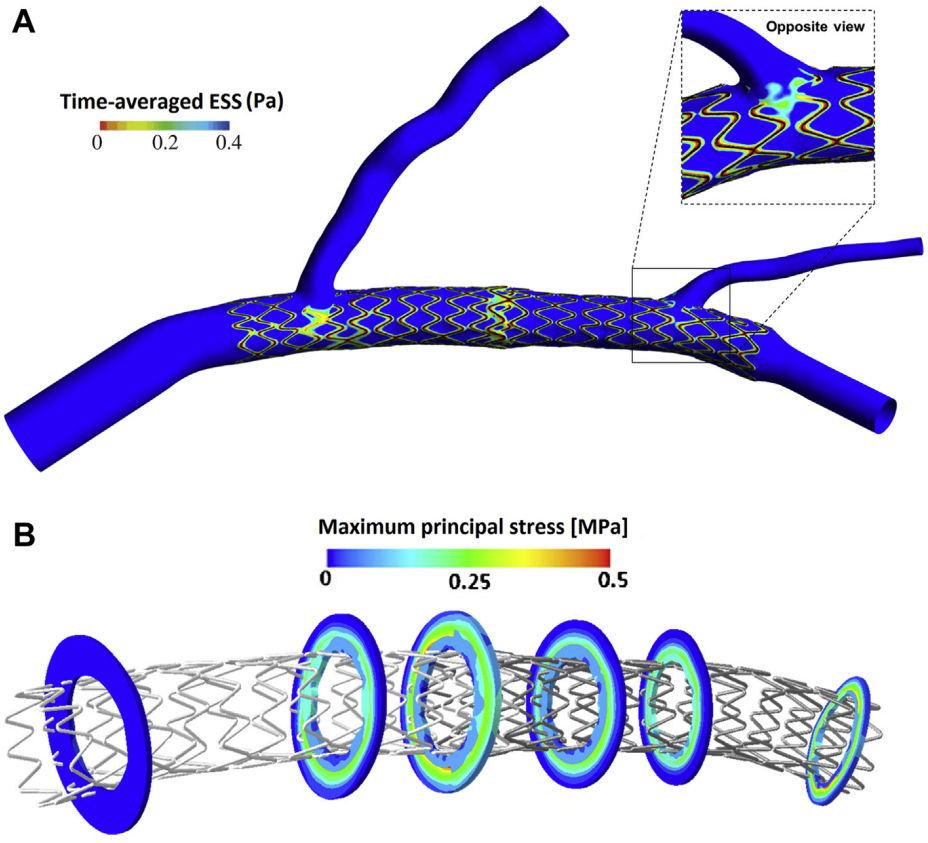

Three-dimensional reconstruction of a stented left anterior descending artery including the diagonal branches using fusion of invasive coronary angiography and cardiac computed tomography angiography. **(A)** Endothelial shear stress (ESS) distribution in the reconstructed arteries using computational fluid dynamics (low ESS is denoted in **red**). **(B)** Maximum principal stresses within the arterial wall of the stented segment. Reprinted with permission from Chiastra et al. (18) and Morlacchi et al. (19). MPa = Megapascal; Pa = Pascal.

assessment of coronary lesions in the catheterization laboratory. Such modeling techniques may also be applicable to other vascular beds, such as the common carotid artery bifurcation or the aortic bifurcation into common iliac arteries, both of which are common locations of atherosclerosis. Joint efforts across multidisciplinary teams of interventional cardiologists, biomedical engineers, and molecular biologists are anticipated to facilitate the effective integration of rapidly emerging novel technologies into clinical practice. In the challenging pursuit of percutaneous treatment of bifurcation lesions, modeling and simulation methods provide the opportunity to translate biomechanical engineering breakthroughs into quantifiable and patient-oriented clinical benefits.

REPRINT REQUESTS AND CORRESPONDENCE: Dr. Yiannis S. Chatzizisis, Cardiovascular Division, Brig-ham and Women'sHospital, Harvard Medical School, 75 Francis Street, Boston, Massachusetts 02115. E-mail: ychatzizisis@icloud.com.

PERSPECTIVES

WHAT IS KNOWN? A large proportion of atherosclerotic plaques develop in coronary bifurcations, and stenting in these regions carries higher risk for in-stent restenosis, thrombosis, and recurrent clinical events. Computer simulations and in vitro bench testing can yield incremental information to the anatomical and functional assessment of bifurcation lesions in the catheterization laboratory, thereby guiding percutaneous therapeutic strategies.

WHAT IS NEW? Biomechanical modeling can be particularly useful in the study of stent behavior and stent-wall interactions, optimization of stenting techniques, and development of new generation stents, ultimately improving clinical outcomes.

WHAT IS NEXT? Large-scale clinical studies are warranted to investigate the translation of biomechanical modeling to daily clinical practice.

REFERENCES

1. Lassen JF, Holm NR, Stankovic G, et al. Percutaneous coronary intervention for coronary bifurcation disease: consensus from the first 10 years of the European Bifurcation Club meetings. EuroIntervention 2014;10:545–60.

2. Nakazawa G, Yazdani SK, Finn AV, Vorpahl M, Kolodgie FD, Virmani R. Pathological findings at bifurcation lesions: the impact of flow distribution on atherosclerosis and arterial healing after stent implantation. J Am Coll Cardiol 2010;55: 1679–87.

3. Colombo A, Moses JW, Morice MC, et al. Randomized study to evaluate sirolimus-eluting stents implanted at coronary bifurcation lesions. Circulation 2004;109:1244–9.

4. Richter Y, Edelman ER. Cardiology is flow. Circulation 2006;113:2679–82.

5. Chatzizisis YS, Coskun AU, Jonas M, Edelman ER, Feldman CL, Stone PH. Role of endothelial shear stress in the natural history of coronary atherosclerosis and vascular remodeling: molecular, cellular, and vascular behavior. J Am Coll Cardiol 2007;49:2379–93.

6. Koskinas KC, Chatzizisis YS, Antoniadis AP, Giannoglou GD. Role of endothelial shear stress in stent restenosis and thrombosis: pathophysiologic mechanisms and implications for clinical translation. J Am Coll Cardiol 2012;59:1337–49.

7. Koskinas KC, Chatzizisis YS, Baker AB, Edelman ER, Stone PH, Feldman CL. The role of low endothelial shear stress in the conversion of atherosclerotic lesions from stable to unstable plaque. Curr Opin Cardiol 2009;24: 580–90.

8. Giannoglou GD, Antoniadis AP, Koskinas KC, Chatzizisis YS. Flow and atherosclerosis in coronary bifurcations. EuroIntervention 2010;6 Suppl J:J16–23.

9. Antoniadis AP, Giannopoulos AA, Wentzel JJ, et al. Impact of local flow haemodynamics on atherosclerosis in coronary artery bifurcations. EuroIntervention 2015;11 Suppl V:V18–22.

10. Holzapfel GA, Stadler M, Gasser TC. Changes in the mechanical environment of stenotic arteries during interaction with stents: computational assessment of parametric stent designs. J Biomech Eng 2005;127:166–80.

11. Morlacchi S, Migliavacca F. Modeling stented coronary arteries: where we are, where to go. Ann Biomed Eng 2013;41:1428–44.

12. Duraiswamy N, Schoephoerster RT, Moore JE Jr. Comparison of near-wall hemodynamic parameters in stented artery models. J Biomech Eng 2009;131:061006.

13. Foin N, Gutierrez-Chico JL, Nakatani S, et al. Incomplete stent apposition causes high shear flow disturbances and delay in neointimal coverage as a function of strut to wall detachment distance: implications for the management of incomplete stent apposition. Circ Cardiovasc Interv 2014;7:180–9.

14. Migliavacca F, Chiastra C, Chatzizisis YS, Dubini G. Virtual bench testing to study coronary bifurcation stenting. EuroIntervention 2015;11 Suppl V:V31–4.

15. Martin D, Boyle FJ. Computational structural modelling of coronary stent deployment: a review. Comput Methods Biomech Biomed Engin 2011;14: 331–48.

16. Murphy J, Boyle F. Predicting neointimal hyperplasia in stented arteries using time-dependent computational fluid dynamics: a review. Comput Biol Med 2010;40:408–18.

17. Gijsen FJ, Migliavacca F, Schievano S, et al. Simulation of stent deployment in a realistic human coronary artery. Biomed Eng Online 2008;7:23.

18. Chiastra C, Morlacchi S, Gallo D, et al. Computational fluid dynamic simulations of image-based stented coronary bifurcation models. J R Soc Interface 2013;10:20130193.

19. Morlacchi S, Colleoni SG, Cardenes R, et al. Patient-specific simulations of stenting procedures in coronary bifurcations: two clinical cases. Med Eng Phys 2013;35:1272–81.

20. Gundert TJ, Shadden SC, Williams AR, Koo BK, Feinstein JA, Ladisa JF Jr. A rapid and computationally inexpensive method to virtually implant current and next-generation stents into subject-specific computational fluid dynamics models. Ann Biomed Eng 2011;39:1423–37.

21. Ellwein LM, Otake H, Gundert TJ, et al. Optical coherence tomography for patient-specific 3D artery reconstruction and evaluation of wall shear stress in a left circumflex coronary artery. Cardiovasc Eng Technol 2011;2:212–27.

22. Chiastra C, Morlacchi S, Pereira S, Dubini G, Migliavacca F. Computational fluid dynamics of stented coronary bifurcations studied with a hybrid discretization method. Eur J Mech B/Fluids 2012;35:76–84.

23. De Santis G, De Beule M, Segers P, Verdonck P, Verhegghe B. Patient-specific computational haemodynamics: generation of structured and conformal hexahedral meshes from triangulated surfaces of vascular bifurcations. Comput Methods Biomech Biomed Engin 2011;14:797–802.

24. Loree HM, Grodzinsky AJ, Park SY, Gibson LJ, Lee RT. Static circumferential tangential modulus of human atherosclerotic tissue. J Biomech 1994; 27:195–204.

25. Akyildiz AC, Speelman L, Gijsen FJ. Mechanical properties of human atherosclerotic intima tissue. J Biomech 2014;47:773–83.

26. Zhao S, Gu L, Froemming SR. Finite element analysis of the implantation of a self-expanding stent: impact of lesion calcification. J Med De-vices 2012;6:21001.

27. Pericevic I, Lally C, Toner D, Kelly DJ. The influence of plaque composition on underlying arterial wall stress during stent expansion: the case for lesion-specific stents. Med Eng Phys 2009;31:428–33.

28. Gastaldi D, Morlacchi S, Nichetti R, et al. Modelling of the provisional side-branch stenting approach for the treatment of atherosclerotic coronary bifurcations: effects of stent positioning. Biomech Model Mechanobiol 2010;9:551–61.

29. Mortier P. Computer Modelling of Coronary Bifurcation Stenting. Ghent, Belgium: Ghent University, 2010.

30. Kolandaivelu K, Leiden BB, Edelman ER. Predicting response to endovascular therapies: dissecting the roles of local lesion complexity, systemic comorbidity, and clinical uncertainty. J Biomech 2014;47:908–21.

31. Morlacchi S, Chiastra C, Cutri E, et al. Stent deformation, physical stress, and drug elution obtained with provisional stenting, conventional culotte and Tryton-based culotte to treat bifurcations: a virtual simulation study. EuroIntervention 2014;9:1441–53.

32. Duraiswamy N, Jayachandran B, Byrne J, Moore JE Jr., Schoephoerster RT. Spatial distri-bution of platelet deposition in stented arterial models under physiologic flow. Ann Biomed Eng 2005;33:1767–77.

33. Tzafriri AR, Vukmirovic N, Kolachalama VB, Astafieva I, Edelman ER. Lesion complexity determines arterial drug distribution after local drug delivery. J Control Release 2010;142:332–8.

34. Cutri E, Zunino P, Morlacchi S, Chiastra C, Migliavacca F. Drug delivery patterns for different stenting techniques in coronary bifurcations: a comparative computational study. Biomech Model Mechanobiol 2013;12:657–69.

35. Mortier P, De Beule M, Van Loo D, Verhegghe B, Verdonck P. Finite element analysis of side branch access during bifurcation stenting. Med Eng Phys 2009;31:434–40.

36. Guerin P, Pilet P, Finet G, et al. Drug-eluting stents in bifurcations: bench study of strut deformation and coating lesions. Circ Cardiovasc Interv 2010;3:120–6.

37. Basalus MW, van Houwelingen KG, Ankone MJ, Feijen J, von Birgelen C. Micro-computed tomographic assessment following extremely oversized partial postdilatation of drug-eluting stents. EuroIntervention 2010;6:141–8.

38. Murasato Y. Bench testing of coronary bifurcation stenting techniques: How is it done? Does it help technical decision making? In: Moussa ID, Colombo A, editors. Tips and Tricks in Interventional Therapy of Coronary Bifurcation Lesions. location. London, UK: Informa Healthcare, 2010: 193–210.

39. Hildick-Smith D, Lassen JF, Albiero R, et al. Consensus from the 5th European Bifurcation Club meeting. EuroIntervention 2010;6:34–8.

40. Mortier P, Hikichi Y, Foin N, et al. Provisional stenting of coronary bifurcations: insights into final kissing balloon post-dilation and stent design by computational modeling. J Am Coll Cardiol Intv 2014;7:325–33.

41. Morlacchi S, Chiastra C, Gastaldi D, Pennati G, Dubini G, Migliavacca F. Sequential structural and fluid dynamic numerical simulations of a stented bifurcated coronary artery. J Biomech Eng 2011; 133:121010.

42. Basmadjian D. The effect of flow and mass transport in thrombogenesis. Ann Biomed Eng 1990;18:685–709.

43. Kolandaivelu K, Swaminathan R, Gibson WJ, et al. Stent thrombogenicity early in high-risk interventional settings is driven by stent design and deployment and protected by polymer-drug coatings. Circulation 2011;123:1400–9.

44. Kolandaivelu K, Edelman ER. Environmental influences on endovascular stent platelet reactivity: an in vitro comparison of stainless steel and gold surfaces. J Biomed Mater Res A 2004;70: 186–93.

45. LaDisa JF Jr., Olson LE, Molthen RC, et al. Alterations in wall shear stress predict sites of neointimal hyperplasia after stent implantation in rabbit iliac arteries. Am J Physiol Heart Circ Physiol 2005;288:H2465–75.

46. Chen HY, Hermiller J, Sinha AK, Sturek M, Zhu L, Kassab GS. Effects of stent sizing on endothelial and vessel wall stress: potential mechanisms for in-stent restenosis. J Appl Physiol (1985) 2009;106:1686–91.

47. Gijsen FJ, Oortman RM, Wentzel JJ, et al. Usefulness of shear stress pattern in predicting neointima distribution in sirolimus-eluting stents in coronary arteries. Am J Cardiol 2003;92:1325–8.

48. Jimenez JM, Davies PF. Hemodynamically driven stent strut design. Ann Biomed Eng 2009; 37:1483–94.

49. Sick P, Huttl T, Niebauer J, et al. Influence of residual stenosis after percutaneous coronary intervention with stent implantation on development of restenosis and stent thrombosis. Am J Cardiol 2003;91:148–53.

50. Raber L, Juni P, Loffel L, et al. Impact of stent overlap on angiographic and long-term clinical outcome in patients undergoing drug-eluting stent implantation. J Am Coll Cardiol 2010;55: 1178–88.

51. Kassab GS, Navia JA. Biomechanical considerations in the design of graft: the homeostasis hypothesis. Annu Rev Biomed Eng 2006;8:499–535.

52. Thubrikar MJ, Baker JW, Nolan SP. Inhibition of atherosclerosis associated with reduction of arterial intramural stress in rabbits. Arteriosclerosis 1988;8:410–20.

53. Chen HY, Sinha AK, Choy JS, et al. Mis-sizing of stent promotes intimal hyperplasia: impact of endothelial shear and intramural stress. Am J Physiol Heart Circ Physiol 2011;301:H2254–63.

54. Ormiston JA, Webster MW, El Jack S, et al. Drug-eluting stents for coronary bifurcations: bench testing of provisional side-branch strategies. Catheter Cardiovasc Interv 2006;67:49–55.

55. Foin N, Mattesini A, Ghione M, et al. Tools and techniques clinical: optimising stenting strategy in bifurcation lesions with insights from in vitro bifurcation models. EuroIntervention 2013;9: 885–7.

56. Murasato Y, Horiuchi M, Otsuji Y. Three-dimensional modeling of double-stent techniques at the left main coronary artery bifurcation using micro-focus X-ray computed tomography. Catheter Cardiovasc Interv 2007;70:211–20.

57. Murasato Y, Hikichi Y, Horiuchi M. Examination of stent deformation and gap formation after complex stenting of left main coronary artery bifurcations using microfocus computed tomography. J Interv Cardiol 2009;22:135–44.

58. Ormiston JA, Webster MW, Webber B, Stewart JT, Ruygrok PN, Hatrick RI. The "crush" technique for coronary artery bifurcation stenting: insights from micro-computed tomographic imaging of bench deployments. J Am Coll Cardiol Intv 2008;1:351–7.

59. Murasato Y, Hikichi Y, Nakamura S, et al. Recent perspective on coronary bifurcation intervention: statement of the "Bifurcation Club in KOKURA." J Interv Cardiol 2010;23:295–304.

60. Richter Y, Groothuis A, Seifert P, Edelman ER. Dynamic flow alterations dictate leukocyte adhesion and response to endovascular interventions. J Clin Invest 2004;113:1607–14.

61. Katritsis DG, Siontis GC, Ioannidis JP. Double versus single stenting for coronary bifurcation lesions: a meta-analysis. Circ Cardiovasc Interv 2009;2:409–15.

62. Zimarino M, Corazzini A, Ricci F, Di Nicola M, De Caterina R. Late thrombosis after double versus single drug-eluting stent in the treatment of coronary bifurcations: a meta-analysis of randomized and observational studies. J Am Coll Cardiol Intv 2013;6:687–95.

63. Mortier P, Van Loo D, De Beule M, et al. Comparison of drug-eluting stent cell size using micro-CT: important data for bifurcation stent selection. EuroIntervention 2008;4:391–6.

64. Ormiston JA, Webster MW, Ruygrok PN, Stewart JT, White HD, Scott DS. Stent deformation following simulated side-branch dilatation: a comparison of five stent designs. Catheter Cardiovasc Interv 1999;47:258–64.

65. Foin N, Torii R, Alegria E, et al. Location of side branch access critically affects results in bifurcation stenting: insights from bench modeling and computational flow simulation. Int J Cardiol 2013; 168:3623–8.

66. Alegra-Barrero E, Foin N, Chan PH, et al. Optical coherence tomography for guidance of distal cell recrossing in bifurcation stenting: choosing the right cell matters. EuroIntervention 2012;8: 205–13.

67. Murasato Y, Iwasaki K, Yamamoto T, et al. Optimal kissing balloon inflation after single-stent deployment in a coronary bifurcation model. EuroIntervention 2014;10:934–41.

68. Foin N, Secco GG, Ghilencea L, Krams R, Di Mario C. Final proximal post-dilatation is necessary after kissing balloon in bifurcation stenting. EuroIntervention 2011;7:597–604.

69. Foin N, Torii R, Mortier P, et al. Kissing balloon or sequential dilation of the side branch and main vessel for provisional stenting of bifurcations: lessons from micro-computed tomography and computational simulations. J Am Coll Cardiol Intv 2012;5:47–56.

70. Foin N, Alegria-Barrero E, Torii R, et al. Crush, culotte, T and protrusion: which 2-stent technique for treatment of true bifurcation lesions? insights from in vitro experiments and micro-computed tomography. Circ J 2013;77:73–80.

71. Mitsouras D, Liacouras P, Imanzadeh A, et al. Medical 3D printing for the radiologist. Radio-Graphics 2015. In press.

72. Kralev S, Haag B, Spannenberger J, et al. Expansion of the Multi-Link Frontier coronary bifurcation stent: micro-computed tomographic assessment in human autopsy and porcine heart samples. PLoS One 2011;6:e21778.

73. Toutouzas K, Chatzizisis YS, Riga M, et al. Accurate and reproducible reconstruction of coronary arteries and endothelial shear stress calculation using 3D OCT: comparative study to 3D IVUS and 3D QCA. Atherosclerosis 2015;240:510–9.

74. Cardenes R, Diez JL, Larrabide I, Bogunovic H, Frangi AF. 3D modeling of coronary artery bifurcations from CTA and conventional coronary angiography. Med Image Comput Comput Assist Interv 2011;14:395–402.

75. Giannoglou GD, Chatzizisis YS, Sianos G, et al. In-vivo validation of spatially correct three-dimensional reconstruction of human coronary arteries by inte-grating intravascular ultrasound and biplane angi-ography. Coron Artery Dis 2006;17:533–43.

76. Tu S, Holm NR, Koning G, Huang Z, Reiber JH. Fusion of 3D QCA and IVUS/OCT. Int J Cardiovasc Imaging 2011;27:197–207.

77. Mortier P, Wentzel JJ, De Santis G, et al. Patient-specific computer modelling of coronary bifurcation stenting: the John Doe programme. EuroIntervention 2015;11 Suppl V:V35–9.

78. Antoniadis AP, Jaguszewski M, Maier W, Giannoglou GD, Luscher TF, Templin C. Geometrically correct three-dimensional optical coherence tomography: first self-expanding bifurcation stent evaluation. Eur Heart J 2013;34:2715.

79. Tu S, Pyxaras SA, Li Y, Barbato E, Reiber JH, Wijns W. In vivo flow simulation at coronary bifurcation reconstructed by fusion of 3-dimensional X-ray angiography and optical coherence tomog-raphy. Circ Cardiovasc Interv 2013;6:e15–7.

80. Karanasos A, Li Y, Tu S, et al. Is it safe to implant bioresorbable scaffolds in ostial side-branch lesions? Impact of 'neo-carina' formation on main-branch flow pattern. Longitudinal clinical observations. Atherosclerosis 2015;238:22–5.

81. Ramkumar PG, Mitsouras D, Feldman CL, Stone PH, Rybicki FJ. New advances in cardiac computed tomography. Curr Opin Cardiol 2009; 24:596–603.

82. Luo T, Wischgoll T. Kwon Koo B, Huo Y, Kassab GS. IVUS validation of patient coronary artery lumen area obtained from CT images. PLoS One 2014;9:e86949.